29. *Investigation on the Deformation of the Earth's Crust in Idu Peninsula connected with the Idu Earthquake of Nov. 26, 1930.*

By Chûji TSUBOI,

Earthquake Research Institute.

(Read March 15, 1932.—Received March 20, 1932.)

On Nov. 26, 1930, a destructive earthquake occurred in Idu Peninsula resulting the loss of 259 lives. In many respects this earthquake afforded a number of problems of great scientific interest. This was especially so from the geological point of view as a remarkable seismic fault, the Tanna fault, appeared with the earthquake that was right along the well-known tectonic line through the middle of the peninsula. The deformation of the earth's crust in this district connected with the earthquake is thus one of the most important clues for elucidating the mechanism of the occurrence of the earthquake. In his previous paper,[1] the writer discussed the results of the comparison of the old and new precise levellings made around the peninsula. In the present paper will be given the dicussions on the results of the comparison of the old and new triangulations over the meizoseismal area. The revision of the triangulation in this area was entrusted by Prof. K. Suyehiro, the director of our Institute, to the Land Survey Department of the Imperial Army which accomplished the work recently. The results of the present triangulation were compared with the older one made immediately after the Kwanto earthquake of 1923 and large displacements of the triangulation points were found, most part of which is to be regarded to have been produced connected with the Idu earthquake.

For the present survey, a base line of 1 km. length was newly established in the plain in the neighbourhood of Daiba and the new survey was referred to this. For comparing the old and new geodetic coordinates of the triangulation points, it was assumed that the geodetic position of Asitakayama and the azimuth of the line from Asitakayama to Kamurigadake remained unchanged notwithstanding the disturbances of the

1) C. TSUBOI, *Bull. Earthq. Res. Inst.*, 9 (1931), 271.

earthquake. These assumptions are of course of a tentative nature but so far as we confine ourselves to the discussion of the relative displacements of the triangulation points and the strain on the earth's crust produced by them, they will produce no serious effect on the results of calculation based on it. Similar assumptions have also been necessary in the calculation of the strains in other districts. The effects of these assumptions can easily be considered in the following manner.

Let in Fig. 1, ABC be a triangle before the earthquake disturbance of which AB is assumed to be unchanged both in its length and direction. Let $A'B'C'$ be the true position of the triangle after the disturbance which however we do not know. We have assumed $AB=A'B'$ and $\theta=\theta'$. The error in position of the point C that is produced by this untrue comparison is given as follows:

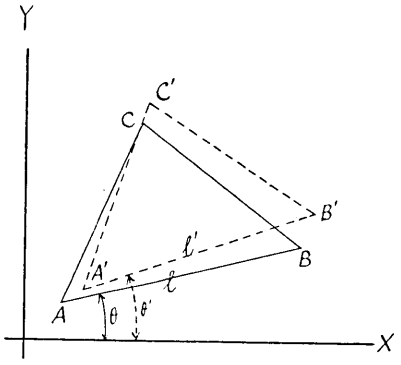

Fig. 1.

$$u=U+u_0+x\frac{d(AB)}{AB}-(\theta-\theta')y,$$

$$v=V+v_0+y\frac{d(AB)}{AB}+(\theta-\theta')x,$$

where U and V are x-, y-components of real displacement of C, u and v those on unreal assumptions, u_0 and v_0, x-, y- components of displacement of the point A, and x and y are the relative co-ordinates of the point C with respect to A. Let AB be denoted by l and $(\theta-\theta')$ by $d\theta$, then

$$\begin{cases} u=U+u_0+x\dfrac{dl}{l}-yd\theta, \\ v=V+v_0+y\dfrac{dl}{l}+xd\theta. \end{cases}$$

If we calculate the strains from these values, we get

$$\begin{cases} \dfrac{\partial u}{\partial x}=\dfrac{\partial U}{\partial x}+\dfrac{dl}{l}, \\ \dfrac{\partial u}{\partial y}=\dfrac{\partial U}{\partial y}-d\theta, \end{cases}$$

$$\begin{cases} \dfrac{\partial v}{\partial x}=\dfrac{\partial V}{\partial x}+d\theta, \\ \dfrac{\partial v}{\partial y}=\dfrac{\partial V}{\partial y}+\dfrac{dl}{l}. \end{cases}$$

$$\begin{cases} \dfrac{\partial u}{\partial x}+\dfrac{\partial v}{\partial y}=\left(\dfrac{\partial U}{\partial x}+\dfrac{\partial V}{\partial y}\right)+2\dfrac{dl}{l} & \ldots\text{dilatation}, \\ \dfrac{1}{2}\left(\dfrac{\partial u}{\partial y}-\dfrac{\partial v}{\partial x}\right)=\dfrac{1}{2}\left(\dfrac{\partial U}{\partial x}-\dfrac{\partial V}{\partial x}\right)-d\theta & \ldots\text{rotation}, \\ \dfrac{1}{2}\left(\dfrac{\partial u}{\partial y}+\dfrac{\partial v}{\partial y}\right)=\dfrac{1}{2}\left(\dfrac{\partial U}{\partial y}+\dfrac{\partial V}{\partial x}\right) & \ldots\text{shear}. \end{cases}$$

$$\sigma=\sqrt{\left(\frac{\partial u}{\partial x}-\frac{\partial v}{\partial y}\right)^2+\left(\frac{\partial v}{\partial x}+\frac{\partial u}{\partial y}\right)^2}=\sqrt{\left(\frac{\partial U}{\partial x}-\frac{\partial V}{\partial y}\right)^2+\left(\frac{\partial V}{\partial x}+\frac{\partial U}{\partial y}\right)^2}$$

....maximum shear.

$$\gamma_{1,2}=\left(\frac{\partial u}{\partial x}+\frac{\partial v}{\partial y}\right)\pm\sqrt{\left(\frac{\partial u}{\partial x}-\frac{\partial V}{\partial y}\right)^2+\left(\frac{\partial u}{\partial y}+\frac{\partial v}{\partial x}\right)^2}$$

$$=\left(\frac{\partial U}{\partial x}+\frac{\partial V}{\partial y}\right)\pm\sqrt{\left(\frac{\partial U}{\partial x}-\frac{\partial V}{\partial y}\right)^2+\left(\frac{\partial V}{\partial x}+\frac{\partial U}{\partial y}\right)^2}+2\frac{dl}{l}$$

....principal strain.

$$\tan\theta_{1,2}=\frac{\gamma_{1,2}-2\dfrac{\partial u}{\partial x}}{\dfrac{\partial u}{\partial y}+\dfrac{\partial v}{\partial x}}=\frac{\left(\dfrac{\partial U}{\partial x}+\dfrac{\partial V}{\partial y}\right)\pm\sqrt{\left(\dfrac{\partial U}{\partial x}+\dfrac{\partial V}{\partial y}\right)^2+\left(\dfrac{\partial V}{\partial x}+\dfrac{\partial U}{\partial y}\right)^2}-2\dfrac{\partial U}{\partial x}}{\dfrac{\partial U}{\partial y}+\dfrac{\partial V}{\partial x}}$$

... direction of axes of strain ellipse.

Therefore we see that dilatation and rotation and principal strains calculated from the untrue assumption differ from the real ones by a constant term. On the other hand, shear, maximum shear and the direction of the principal axes of strain are just as same as the real ones. Thus the relative distribution of dilatation, rotations and the principal strain are by no means affected by the untrue assumptions, which will only cause some shifts of zero lines.

The displacements of the triangulation points in this district as found by the comparison of their old and new geodetic coordinates are shown in Table I and in Fig. 2.

Table I.

Horizontal Displacements of Triangulation Points in Idu Peninsula.

d Resultant Displacement in cm.
θ Azimuth of Displacement Measured Clockwise from North
u Eastward Component of Displacement in cm.
v Northward Component of Displacement in cm.

	d	θ	u	v
(1) Asitakayama	—	—	—	—
(2) Kamurigadake	29	79°1′	28·5	5·5
(3) Sano-mura	36	170°11′	6·1	−35·5
(4) Miyakami-mura	44	12°15′	9·3	43·0
(5) Manaduru-zaki	64	84°29′	63·7	6·2
(6) Negoya-mura	16	275°31′	−15·9	1·5
(7) Daiba-mura	71	175°54′	5·1	−70·8
(8) Kurodake	99	17°27′	29·7	94·4
(9) Tokurayama	57	225°33′	−40·7	−39·9
(10) Hasima	20	100°36′	19·7	− 3·7
(11) Osaka-mura	121	223°49′	−83·8	−87·3
(12) Sukumoyama	37	357°39′	− 1·5	37·0
(13) Enasi-mura	105	252°20′	−100·0	−31·9

From these values, the dilatation, rotation and shear were calculated for different triangles following the method, due initially to Prof. T. Terada.[2)]

Consider a triangle of which the vertices are of the co-ordinates (x_1y_1), (x_2y_2) and (x_3y_3). Let the horizontal displacements of these points be (u_1v_1), (u_2v_2) and (u_3v_3) and further assume u and v inside the triangle are given by the following expressions

$$u=ax+by+c,$$
$$v=a'x+b'y+c'$$

subjected to the conditions

$$u_{1,2,3}=ax_{1,2,3}+by_{1,2,3}+c,$$
$$v_{1,2,3}=a'x_{1,2,3}+b'y_{1,2,3}+c'.$$

Then
$$\frac{\partial u}{\partial x}=a=\frac{(y_3-y_1)(u_2-u_1)-(y_2-y_1)(u_3-u_1)}{\Delta},$$

2) T. TERADA and N. MIYABE, *Bull. Earthq. Res Inst.*, **7** (1929), 223.

$$\frac{\partial u}{\partial y}=b=\frac{(x_2-x_1)(u_3-u_1)-(x_3-x_1)(u_2-u_1)}{\Delta},$$

$$\frac{\partial v}{\partial x}=a'=\frac{(y_3-y_1)(v_2-v_1)-(y_2-y_1)(v_3-v_1)}{\Delta},$$

$$\frac{\partial v}{\partial y}=b'=\frac{(x_2-x_1)(v_3-v_1)-(x_3-x_1)(v_2-v_1)}{\Delta},$$

where $$\Delta=(x_2-x_1)(y_3-y_1)-(x_3-x_1)(x_2-x_1).$$

The values obtained in this way were taken to be those of the geometrical centre of the triangle. This is the first approximation. Then we can calculate the dilatation, rotation, shear, maximum shear, principal strain, direction of the axes of strain ellipse for different triangles. The results of the calculations are given in Table II and Figs. 3-9.

Table II.

I Triangles. Numerals in the brackets correspond to the triangulation points given in Table I.

II Eastward Gradient of Eastward Displacement $\frac{\partial u}{\partial x}$ in 10^{-5}.

III Northward Gradient of Eastward Displacement $\frac{\partial u}{\partial y}$ in 10^{-5}.

IV Eastward Gradient of Northward Displacement $\frac{\partial v}{\partial x}$ in 10^{-5}.

V Northward Gradient of Northward Displacement $\frac{\partial v}{\partial y}$ in 10^{-5}.

VI Dilatation $\left(\frac{\partial u}{\partial x}+\frac{\partial v}{\partial y}\right)$ in 10^{-5}.

VII Rotation $\frac{1}{2}\left(\frac{\partial u}{\partial y}-\frac{\partial v}{\partial x}\right)$ in 10^{-5}.

VIII Shear $\frac{1}{2}\left(\frac{\partial u}{\partial y}+\frac{\partial v}{\partial x}\right)$ in 10^{-5}.

IX Maximum Shear $\sqrt{\left(\frac{\partial u}{\partial x}-\frac{\partial v}{\partial y}\right)^2+\left(\frac{\partial v}{\partial x}+\frac{\partial u}{\partial y}\right)^2}$ in 10^{-5}.

X Principal Strain $\gamma_1=\left(\frac{\partial u}{\partial x}+\frac{\partial v}{\partial y}\right)+\sqrt{\left(\frac{\partial u}{\partial x}-\frac{\partial v}{\partial y}\right)^2+\left(\frac{\partial u}{\partial y}+\frac{\partial v}{\partial x}\right)^2}$ in 10^{-5}.

XI „ $\gamma_2=\left(\frac{\partial u}{\partial x}+\frac{\partial v}{\partial u}\right)-\sqrt{\left(\frac{\partial u}{\partial x}-\frac{\partial v}{\partial y}\right)^2+\left(\frac{\partial u}{\partial y}+\frac{\partial v}{\partial x}\right)^2}$ in 10^{-5}.

XII Direction of One of the Principal Axes of Strain γ_1

$$\theta=\tan^{-1}\left(\frac{\left(\frac{\partial u}{\partial x}+\frac{\partial v}{\partial y}\right)+\sqrt{\left(\frac{\partial u}{\partial x}-\frac{\partial v}{\partial y}\right)^2+\left(\frac{\partial u}{\partial y}+\frac{\partial v}{\partial x}\right)^2-2\frac{\partial u}{\partial x}}}{\frac{\partial u}{\partial y}+\frac{\partial v}{\partial x}}\right)$$

I	II	III	IV	V	VI	VII	VIII	IX	X	XI	XII
(5)(10)(12)	+0·05	+0·39	−0·36	+0·03	+0·08	+0·38	+0·02	+0·03	+0·11	+0·05	22°
(7) (8)(12)	+0·55	+0·43	+2·76	+0·89	+1·44	−1·17	+1·57	+3·22	+4·64	−1·77	48°
(4) (3) (8)	+0·02	−0·25	+0·82	−0·61	−0·59	−0·54	+0·29	+0·85	+0·26	−1·43	21°
(11) (9)(12)	+0·90	+0·93	+1·32	+1·15	+2·04	−0·20	+1·13	+2·27	+4·32	−0·23	48°
(2) (7) (4)	−0·09	+0·22	+1·89	−0·31	−0·40	−0·84	+1·05	+2·11	+1·72	−2·51	42°
(9)(13)(11)	+0·12	+0·66	−0·55	+0·48	+0·60	+0·60	+0·06	+0·38	+0·98	0·22	81°
(3) (7) (4)	+0·08	+0·04	+0·92	+1·06	+1·09	−0·44	+0·46	+1·40	+2·49	−0·31	68°
(1) (3) (6	+0·17	+0·26	−0·36	−0·03	+0·15	+0·31	−0·05	+0·22	+0·37	−0·08	167°
(1) (3) (2)	+0·13	+0·15	−0·08	+0·59	+0·72	+0·11	+0·04	+0·47	+1·38	+0·25	86°
(7) (9) (8)	+0·57	+0·48	+1·04	−2·78	−2·21	−0·29	+0·76	+3·67	+1·47	−5·88	11°
(7) (8)(11)	+0·67	+0·69	+2·13	−0·45	+0·23	−0·72	+1·41	+3·03	+3·25	−2·80	34°
(2) (3) (7)	+0·17	+0·10	−0·10	+0·61	+0·78	+0·10	−0·01	+0·44	+1·22	0·34	91°
(1) (6) (9)	−0·10	+0·26	−0·59	−0·03	−0·13	+0·42	−0·17	+0·34	+0·22	−0·47	121°
(7)(12)(11)	+0·86	+0·63	+1·18	−0·18	+0·69	−0·27	+0·90	+2·08	+2·77	−1·40	30°
(3) (7) (8)	+0·45	+0·22	+3·34	+2·13	+2·58	−1·56	+1·78	+3·94	+6·51	−1·36	57°
(2) (4) (5)	+0·53	+0·26	−0·38	−0·46	+0·08	+0·32	−0·06	+2·00	+1·07	−0·92	177°
(12) (8) (5)	+0·04	+0·40	−1·34	+0·64	+0·68	+0·87	−0·47	+1·12	+1·79	−0·44	119°
(4) (8)(10)	−0·17	−0·26	−1·03	−0·66	−0·82	+0·39	−0·64	+1·37	+0·55	−2·19	146°
(5) (4)(10)	+0·54	+0·47	−0·35	+0·03	+0·57	+0·41	+0·06	+0·53	+1·09	−0·05	6°
(9) (8)(12)	+0·57	+0·43	+1·09	+0·79	+1·36	−0·34	+0·76	+1·53	+2·89	−0·18	49°
(6) (3)(13)	+0·12	+0·57	−0·40	+0·26	+0·38	+0·49	+0·09	+0·22	+0·59	+0·16	64°
(11) (6)(13)	+0·12	+0·58	−0·54	+0·26	+0·38	+0·56	+0·02	+0·15	+0·53	+0·24	82°
(1) (7) (3)	+0·09	+0·06	−0·07	+0·63	+0·71	+0·06	−0·01	+0·54	+1·25	+0·17	89°
(6) (9)(13)	+0·20	+0·57	−0·33	+0·25	+0·45	+0·40	+0·12	+0·25	+0·69	+0·20	51°
(9) (7)(11)	+0·41	+0·76	−0·80	+0·39	+0·80	+0·78	−0·02	+0·05	+0·84	+0·76	146°
(2) (3) (4)	+0·05	+0·23	+0·83	−0·38	−0·33	−0·32	+0·53	+1·14	+0·81	−1·47	34°
(4) (8) (5)	+0·51	+0·24	−0·39	−0·64	−0·13	+0·08	−0·31	+1·33	+1·20	−1·46	165°
(1) (9) (7)	+0·51	+0·60	−0·57	−0·02	+0·49	+0·58	+0·02	+0·52	+1·01	−0·03	2°
(9) (8)(11)	+0·58	+0·82	+1·10	+1·07	+1·64	−0·14	+0·96	+1·98	+3·62	−0·34	52°
(6) (3) (9)	+0·13	+0·50	−0·39	+0·19	+0·32	+0·45	+0·06	+0·13	+0·45	+0·19	58°
(7) (3) (9)	+0·67	+0·31	−0·76	+0·32	+0·99	+0·54	−0·23	+0·57	+1·55	+0·42	154°
(8)(10) (5)	+0·05	+0·39	−0·83	−0·05	0	+0·61	−0·22	+0·45	+0·45	−0·45	141°
(8) (4) (7)	+0·24	+0·25	+2·08	−0·57	−0·34	−1·16	+0·92	+2·00	+1·69	−2·34	33°
(8)(12)(10)	+0·05	+0·40	−0·59	+0.69	+0·73	+0·49	−0·10	+0·67	+1·40	−0·06	99°
(11) (8)(12)	+0·84	+0·44	+1·28	+0·80	+1·64	−0·42	+0·86	+1·72	+3·36	−0·69	44°

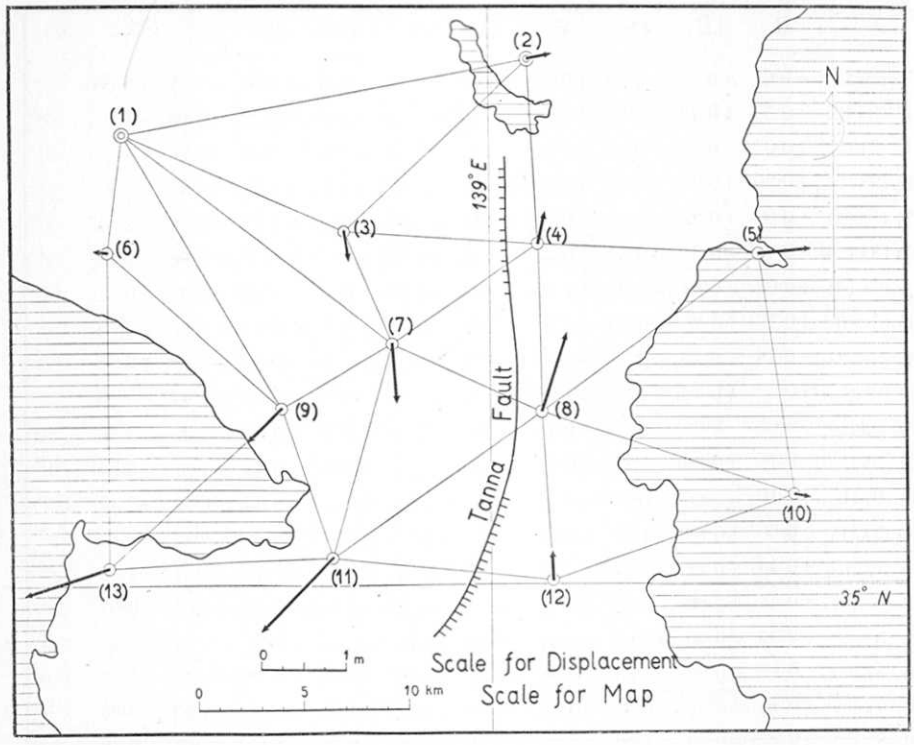

Fig. 2. Horizontal Displacements of the Triangulation Points in Idu Peninsula.

In Fig. 2, the horizontal displacements of the triangulation points are shown by arrows taken to be proportional to their values towards the correspondig directions. It is readily found that the direction of the movement is decidedly opposite on both sides of the Tanna fault. On the western side on the fault, the amount of the displacement is uniformly large throughout, while on its eastern side, they are large only in the immediate neighbourhood of the fault, especially at the point (8). This would seem to indicate that the displacements of the triangulation points on the eastern side of the fault were produced only as a marginal phenomenon. If it is assumed that there was actually some southward component in the displacement of the point (2) then the displacements of the triangulation points on the eastern side of the fault will be of irregular distribution which will be nearly null in their means. In this case, the southwestern displacements of the triangulation points on the western side of the fault will be increased. These circumstances however will not make no influence on the calculation that follows, for which the

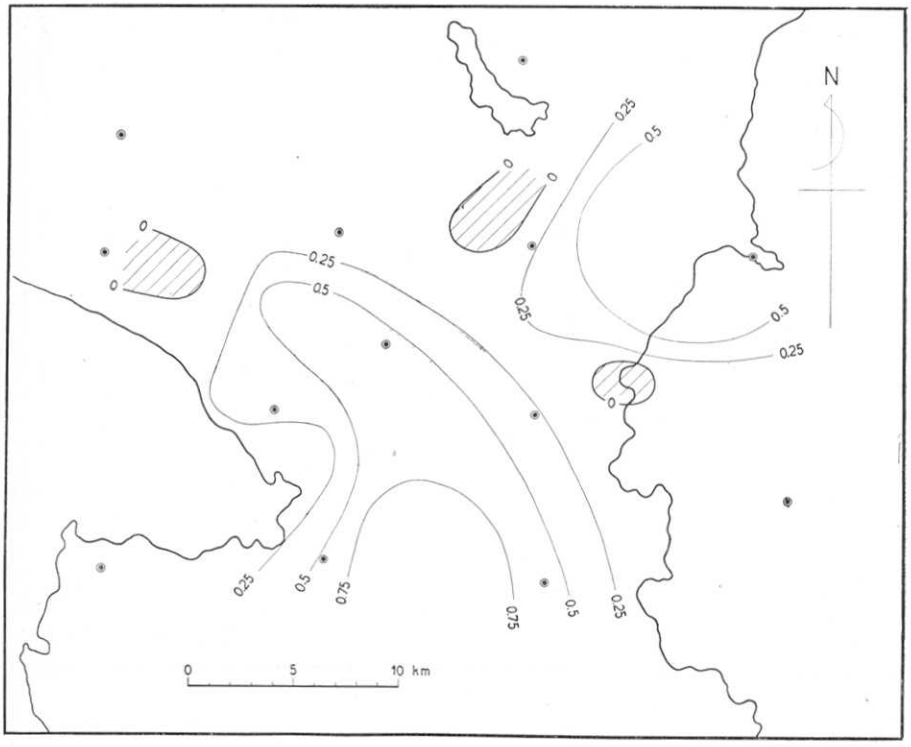

Fig. 3. Lines of Equal Eastward Gradient of Eastward Displacement in 10^{-5}.

reason was proved in the foregoing pages.

In Fig. 3, it is readily seen that the eastward gradient of eastward displacements of the trianglation points are positive almost everywhere in the surveyed area. There is a large difference in amount between them and the northward gradients of northward displacements, which are much larger than the former. The lines of equal eastward gradient of northward displacement in Fig. 4 shows naturally an intimate relation with the trend of the Tanna fault. This quantity is positive along a comparatively narrow zone parallel to the fault. On the eastern and western sides of this zone, the values are negative and their absolute values are much larger on the eastern side than those on the western, which fact indicates that the displacements of the triangulation points on the eastern side of the fault are large only in the immediate neighbourhood of the fault while on its western side the decrease of the amount of horizontal displacement with distance from the fault is very much smaller, the displacements of the triangulation points sensibly far

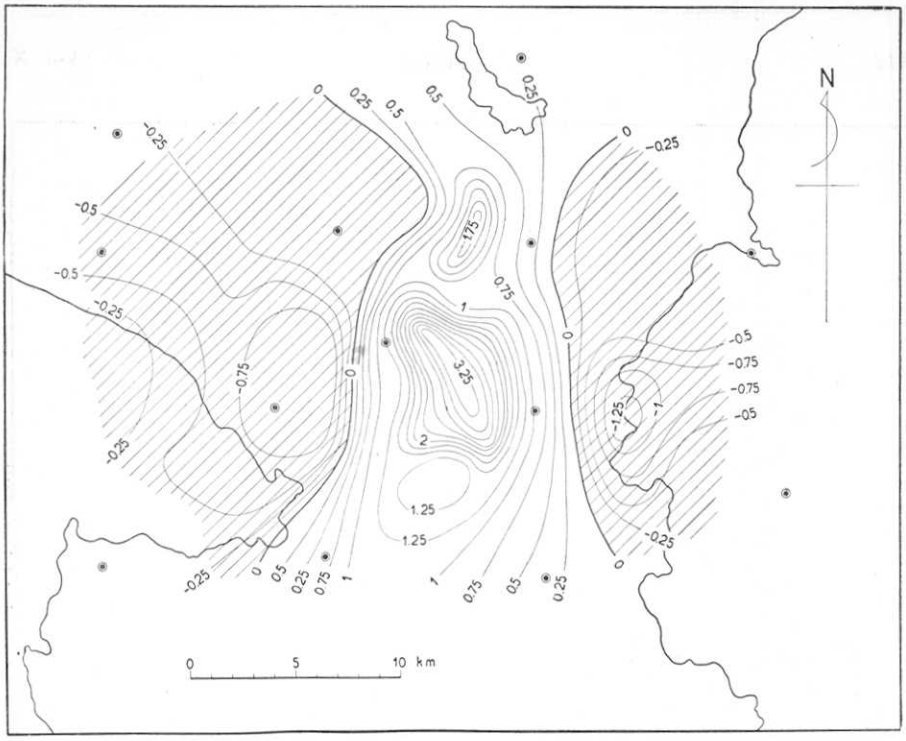

Fig. 4. Lines of Equal Eastward Gradient of Northward Displacement in 10^{-5}.

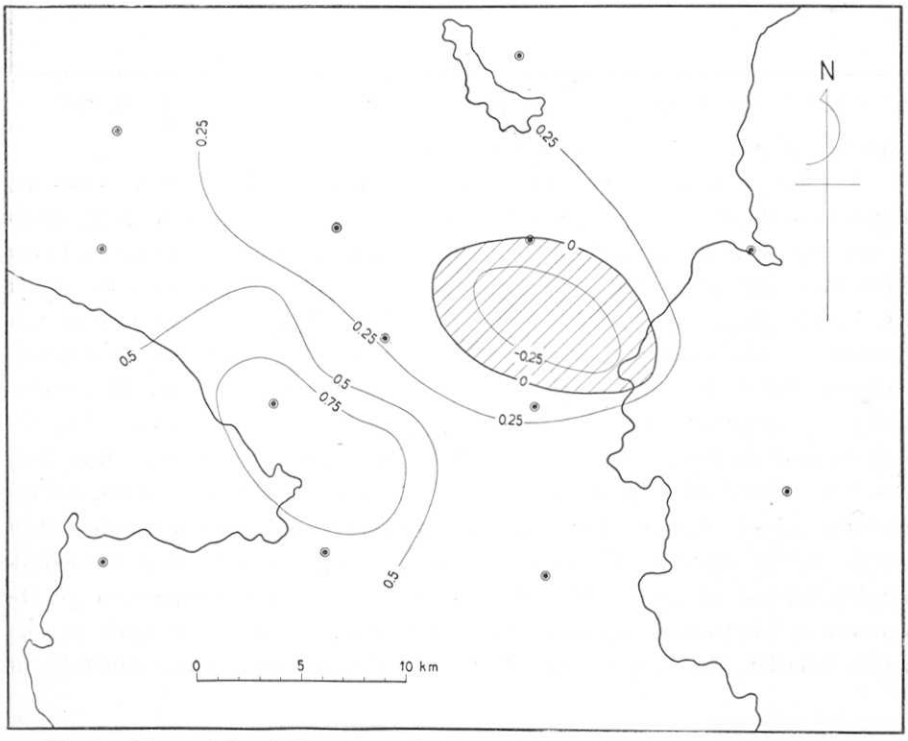

Fig. 5. Lines of Equal Northward Gradient of Eastward Displacement in 10^{-5}.

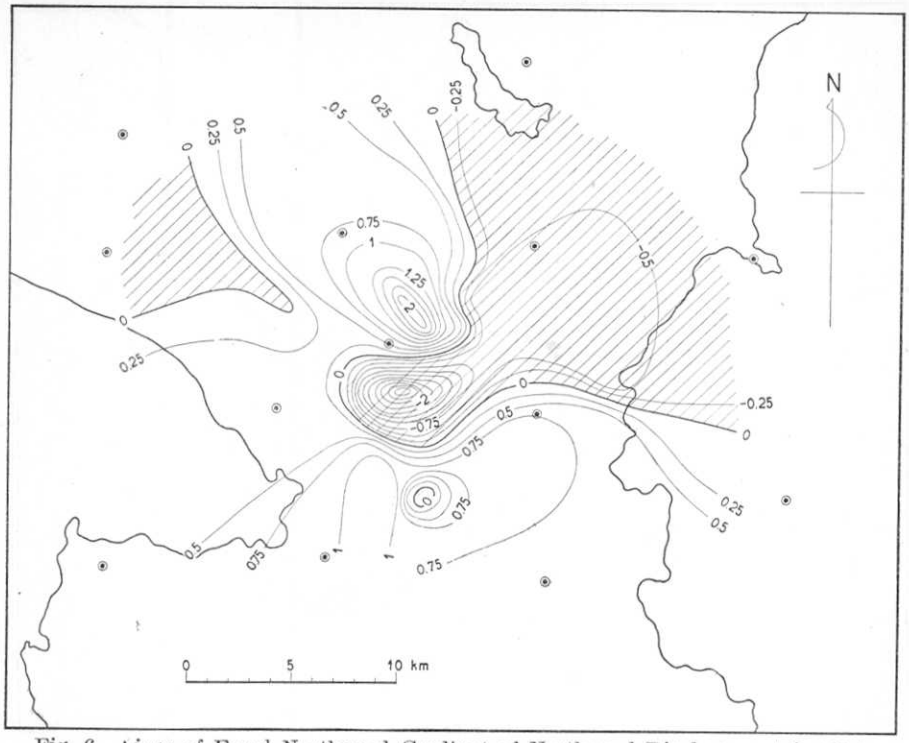

Fig. 6. Lines of Equal Northward Gradient of Northward Displacement in 10^{-5}.

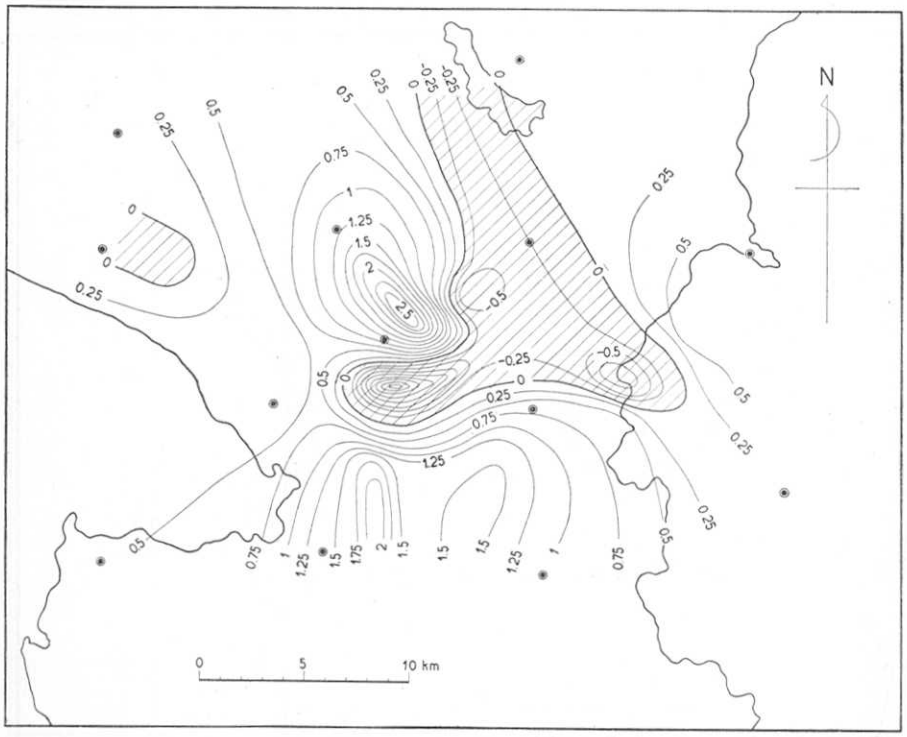

Fig. 7. Lines of Equal Dilatation $\left(\frac{\partial u}{\partial x}+\frac{\partial v}{\partial y}\right)$ in 10^{-5}.

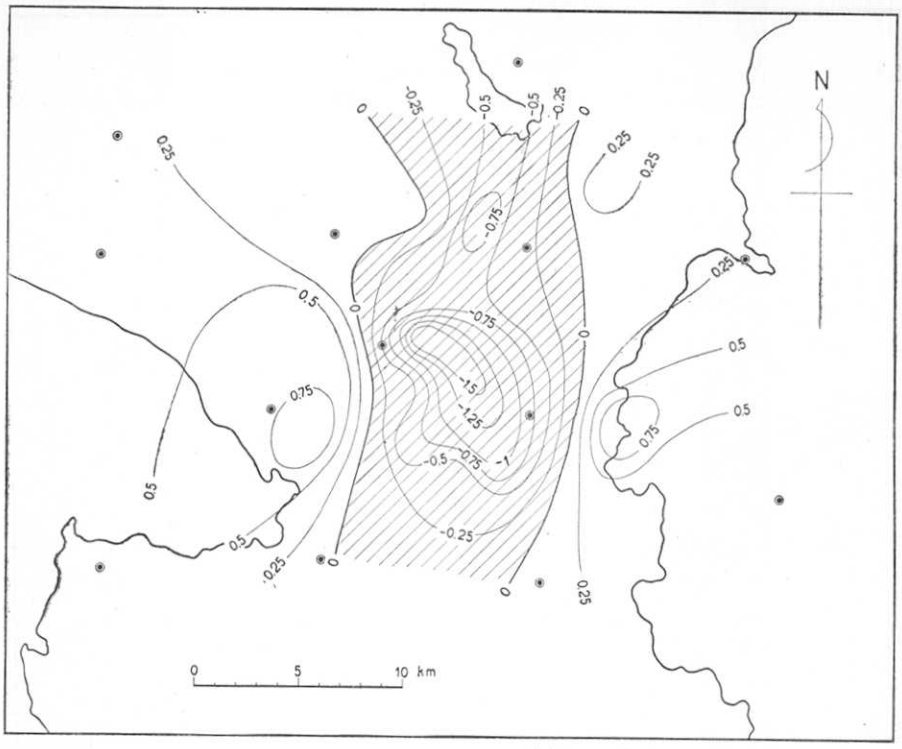

Fig. 8. Lines of Equal Rotation $\frac{1}{2}\left(\frac{\partial u}{\partial y}-\frac{\partial v}{\partial x}\right)$ in 10^{-5}.

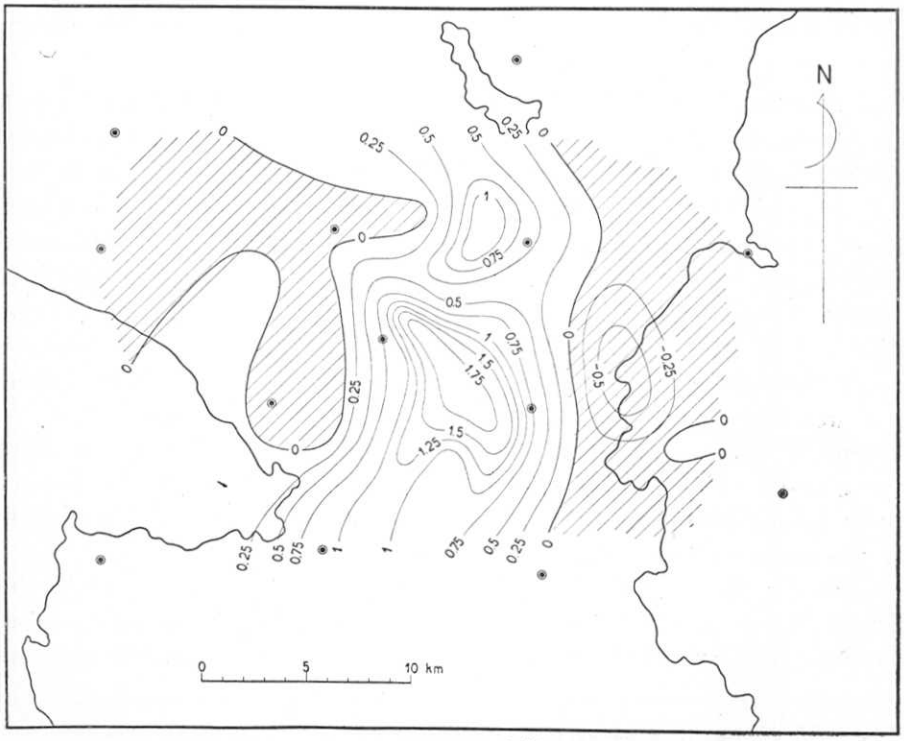

Fig. 9. Lines of Equal Shear $\frac{1}{2}\left(\frac{\partial u}{\partial y}+\frac{\partial v}{\partial x}\right)$ in 10^{-5}.

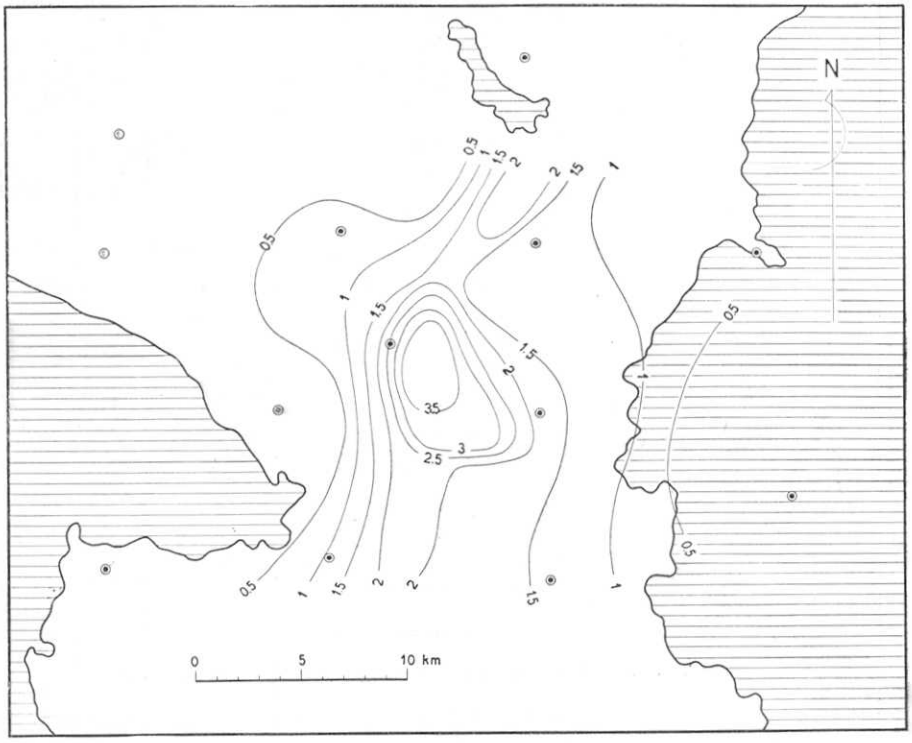

Fig. 10. Lines of Equal Maximum Shear in 10^{-5}.

from the fault nevertheless being large. The values of northward gradient of eastward displacements are very much smaller than those of the eastward gradient of the northward displacement. Thus it seems that the eastward displacements of the triangulation points are not so significant as the northward ones. The northward gradient of the northward displacement shown in Fig. 6 is very large in their amount and it is mainly this that determines the distribution of areal dilatation in the district shown in Fig. 7. The distributions of rotation and shear are nearly the same and this is naturally expected by the smallness of the northward gradient of eastward displacements. The distribution of maximum shear shown in Fig. 10, seems to be interesting in that there are two mutually perpendicular directions along which its value is relatively large. Similar phenomena are also observable with experiments on the rapture of materials.

Finally the distribution of principal axes of strain ellipses in the district shown in Fig. 11 well illustrates the mode of the crust deformations. The principal axes are trending NW-SE and NE-SW and the

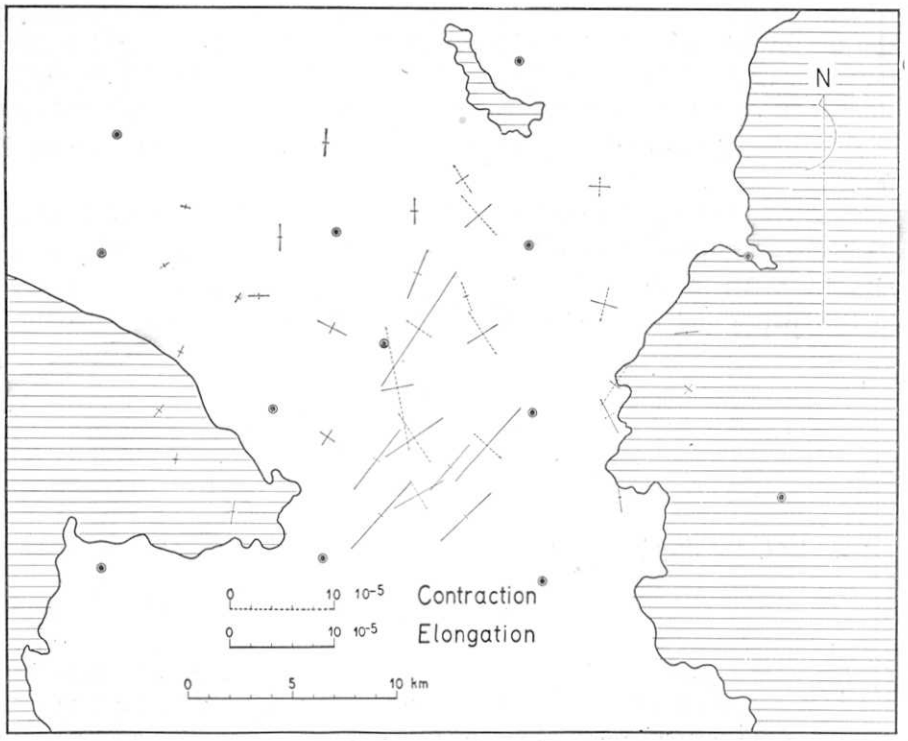

Fig. 11. Principal Axes of Strain Ellipses.

strain ellipses are very much elongated in NE-SW direction in the southern part of the surveyed area. The trend of the Tanna fault is along the direction of maximum shear in its northern part while it is along the direction of maximum elongation in its southern part.

After all, the earth's crust on the western side of the Tanna fault was thus found to have been compressed into SE direction simultaneously with the clockwise rotation and elongation in SW direction. According to H. Tsuya of our Institute, there is a geological evidence that a similar movement of the earth's crust took place in this area in Upper Pleistocene. In his previous paper,[3] on the other hand, the writer showed by the comparison of precise levellings before and after the earthquake that the direction of the tilting of land blocks caused by the earthquake changes itself clockwise as we go from the southern to northern blocks. It was also shown that the block movement of the earth's crust is predominant in that part of the earth's crust in the peninsula that lies on

3) *loc. cit.*

the northwestern part of the Tanna fault which is trending NS in its northern part while gradually SW in its southern part with its convex side to SE. All these facts seem to indicate that the land that did move at the time of the earthquake was that on the northwestern side of the fault.

In conclusion, the writer wishes to express his sincere thanks to Professor Torahika TERADA for his interests in this work. Thanks are also due to Mr. A. JITSUKAWA for his assistance in the calculation involved in this paper and also in the preparation of the figures contained in it.

---

29. 昭和五年伊豆地震に關聯せる伊豆地方の地殻變形に關する研究

地震研究所　坪　井　忠　二

昭和五年十一月二十六日の伊豆地震の後に同地方の三角測量の改測が行はれ、各三角點の移動が明にされたので、其の結果を使つて此の地方の地殻の變形を論じた。此の結果と前に發表した水準測量改測の結果とを綜合して考へると、地震の際に動いたものは丹那斷層の西側の地域であるらしく考へられるのである。
